ACS Macro Letters

Letter

pubs.acs.org/macroletters

Synthesis of pH-Responsive Nanocapsules via Inverse Miniemulsion Periphery RAFT Polymerization and Post-Polymerization Reaction

Robert H. Utama,[†] Markus Drechsler,[‡] Stephan Förster,[§] Per B. Zetterlund,*[,†] and Martina H. Stenzel*[,†,∥]

[†]Centre for Advanced Macromolecular Design (CAMD), School of Chemical Engineering, and [∥]Centre for Advanced Macromolecular Design (CAMD), School of Chemistry, University of New South Wales, Sydney, Australia

[‡]Bayreuth Institute of Macromolecular Research (BIMF) and [§]Physikalische Chemie I, Universität Bayreuth, Bayreuth, Germany

Supporting Information

ABSTRACT: We report herein the versatility of inverse miniemulsion periphery RAFT polymerization (IMEPP) and postpolymerization reaction in producing pH-responsive nanocapsules with different functionalities. The robustness of the polymeric nanocapsules was confirmed by their ability to undergo reactions, be dried, and be redispersed in various solvents without any changes in size and core−shell morphology. Nanocapsules bearing carboxylic acid (COOH) functionalities were produced via hydrolysis, while nanocapsules bearing tertiary-amine (N-X_3) functionalities were synthesized via aminolysis. The responsive behavior of the nanocapsules was tested in aqueous solution with pHs ranging from 3 to 12. Nanocapsules with COOH functionalities were found to swell under basic conditions due to the deprotonated carboxylate ions. In contrast, nanocapsule with tertiary amine functionalities underwent swelling in acidic conditions.

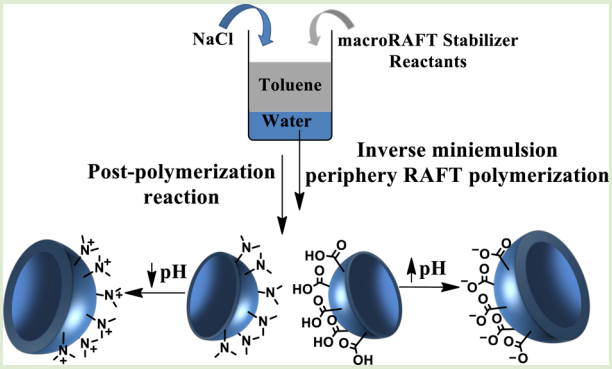

Polymeric nano- and microcapsules responsive to stimuli such as temperature,[1,2] pH,[3−5] magnetic field,[6,7] and redox agents[5,8,9] constitute a growing field of research over the years as they are able to protect and release various molecules on demand. Incorporation of pH-responsive functionalities into linear and complex macromolecules has been explored extensively,[10−12] with the resulting products having potential usage in various fields such as drug delivery,[13,14] sensors,[15,16] and water treatment.[17,18]

Nanocapsules obtained from vesicles are well-documented, which includes the preparation of pH-responsive vesicles.[19,20] Both Chen and co-workers[21] and Song and co-workers[22] have reported the successful self-assembly of amphiphilic copolymers to produce pH responsive vesicles. However, self-assembled nanoparticles are prone to disintegration and structural change upon application in a different environment and, hence, the necessity to incorporate an extra cross-linking step.[23,24] Moreover, the synthesis via self-assembly is generally lacking in control over the size, porosity, and thickness of the shell.

The use of sacrificial templates to obtain nanocapsules is very common. For example, van Herk and co-workers utilized vesicular templates and RAFT polymerization to produce pH-responsive nanocapsules.[25] The use of inorganic sacrificial templates to generate pH responsive polymeric nanocapsules has been frequently reported. This synthetic approach is typically combined with the layer-by-layer (LbL) technique. The resulting polymeric shells are charged and, hence, pH-responsive.[26,27] In contrast to vesicular systems, these nanocapsules are considered to be more stable due to the presence of electrostatic attraction between different layers in solution. Such nanocapsules have also been used as a drug delivery system.[28,29] The pH responsiveness of the shell has also been exploited to not only control the release, but also to achieve efficient encapsulation of guest molecules.[27,30] The most significant limitation of this approach, however, is the complexity of the synthetic steps involved.

Notably absent from the literature are, however, simple self-assembled structures that show simultaneously high structural integrity. Miniemulsion polymerization can be described as a process whereby polymerization is conducted within 50−500 nm droplets dispersed in a continuous phase. It utilizes dispersed liquid droplets as templates for the production of nanocapsules. This method has been used extensively to produce polymeric particles (nanospheres) and more recently, to produce polymeric nanocapsules. One way to produce polymeric nanocapsules is induced-phase separation, whereby the migration of polymers to the interface is promoted by external stimuli. Another approach is through interfacially confined polymerization, such as controlled/living radical polymerization (CLRP),[31,32] polyaddition,[33,34] and click reactions.[35,36] Although the miniemulsion approach offers simplicity, versatility, and control over the size of nanocapsules,

Received: August 15, 2014
Accepted: August 28, 2014
Published: September 4, 2014

   dx.doi.org/10.1021/mz5005019 | *ACS Macro Lett.* 2014, 3, 935−939

currently available methods are still showing issues concerning the generation of solid nanoparticles, lack of control over the shell thickness and reactions (i.e., the polymerization) occurring within the core environment.

To our knowledge, there has only been one report on the production of pH-responsive nanocapsules via the inverse miniemulsion approach. Cao and co-workers[37] performed radical polymerization of *N*-isopropylacrylamide (NIPAM) and 4-vinylpyridine (4-VP, cationic) within the aqueous droplets to produce hydrophobic copolymers, which would then migrate to form the polymeric shell. However, a mixture of nanocapsules and solid nanoparticles were produced. Moreover, the applicability of the method is limited only to water-soluble monomers yielding water insoluble polymers. This was demonstrated when acrylic acid (AA, anionic) was used as the pH responsive group, leading to the generation of solid nanoparticles due to the hydrophilicity of PAA.[37]

We recently reported a method based on the miniemulsion approach referred to as inverse miniemulsion periphery RAFT polymerization (IMEPP) for synthesis of polymeric nanocapsules.[38,39] In this method, amphiphilic block copolymers are used as both stabilizer and macroRAFT agent of a w/o miniemulsion. The self-assembled layer around the water droplets is then stabilized by further chain extension of the diblock copolymer using a divinyl cross-linker. Reported herein is the utilization of IMEPP to produce cationic and anionic pH responsive nanocapsules. This can be achieved by employing amphiphilic block copolymers that can be converted into fully hydrophilic and pH-responsive nanocapsule shells after polymerization (Scheme 1)

Two different macroRAFT stabilizers were used to synthesize pH-responsive nanocapsules. Poly(*N*-(2-hydroxyproyl)methacrylamide) (PHPMA) was chosen as the hydrophilic segment due to its excellent hydrophilicity in addition to its insolubility in the continuous (toluene) phase. The polymerization conversion was 38% from ^{1}H NMR, yielding 16 repeating units. Subsequently, the macroRAFT agent was chain extended separately with two different monomers. Chain extension with *t*-BMA yielded P(*t*BMA) segment with 105 repeating units. Similarly, chain extension with pentafluorophenyl methacrylate (PFPMA) resulted in a P(PFPMA) block with 36 repeating units as determined from ^{19}F NMR (see Supporting Information (SI) for details).

Scheme 1. Schematic Pathway for the Synthesis of Two Different Types of pH-Responsive Nanocapsules via IMEPP and Post-Polymerization Reaction

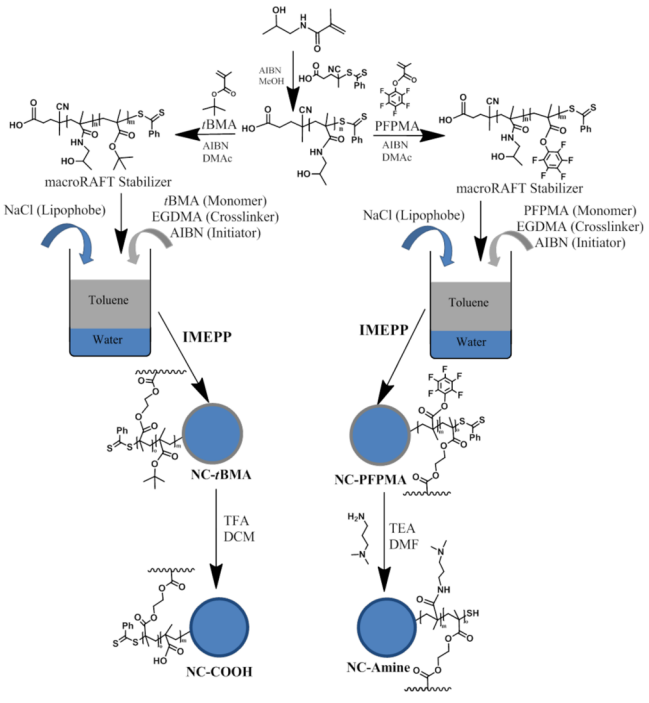

The resulting block copolymers were analyzed using SEC. The resulting traces (SI, Figure S1) showed monomodal distributions for the macroRAFT agent and the block copolymers. The experimentally determined molecular weights from SEC analysis were in good agreement with the theoretically calculated molecular weight (SI, Table S1). The hydrophilic−lipophilic balance (HLB) value of the macroRAFT stabilizers was determined to be suitable for stabilization of an inverse miniemulsion according to the equation described elsewhere[38]

The syntheses of polymeric nanocapsules were conducted via IMEPP, which has been developed by our group.[38,39] Inverse miniemulsions comprising toluene as the continuous phase, water as the dispersed phase, and NaCl as the lipophobe were prepared, with the previously synthesized block copolymers as sole stabilizers (separately). The block copolymers also act as macroRAFT agents for the subsequent interfacial RAFT polymerization. Relevant reactants for the RAFT polymerization were incorporated into the continuous phase (SI, Table S2). RAFT polymerization was then initiated on the outer periphery of the droplets (with the droplets acting as the template), thus, creating polymeric shells that grow outward into the continuous phase. This leaves the droplets interior reaction free, making it potentially useful to encapsulate chemically fragile guest molecules.

To demonstrate the versatility of IMEPP, polymeric nanocapsules with two different shell functionalities were synthesized (Scheme 1). Subsequently, these nanocapsules would undergo different postpolymerization reactions to produce two types of pH-responsive nanocapsules with different responsive behavior over the pH range of 3−12. The first set of polymeric nanocapsules utilized PHPMA-*b*-P*t*BMA stabilizer to produce nanocapsules with P*t*BMA shell (denoted NC-*t*BMA). The second set used PHPMA-*b*-PPFPMA stabilizer to produce nanocapsules with PPFPMA shell (NC-PFPMA) (Scheme 1). Upon sonication, an emulsion with milky appearance was obtained for both systems. The inverse miniemulsions were stable for days as no phase separation was observed. Visual inspection of the inverse miniemulsion droplets was conducted using cryo-TEM. Under cryogenic conditions, the droplets were preserved in their dispersion state, hence, eliminating the disintegration of the morphology that would be experienced under normal TEM conditions. The average diameter of the droplets was in the range of 168−194 nm for NC-PFPMA and 118−149 nm for NC-*t*BMA (Figure 1 and SI, Figure S2). From the micrographs, the thickness of the hydrophobic segment of the stabilizers was estimated to be 6 nm for PPFPMA and 10 nm for P*t*BMA.

From DLS analysis, the droplet diameters (*Z*-avg.) were established to be 206 and 167 nm for NC-PFPMA and NC-*t*BMA, respectively, comparable to the cryo-TEM results (Table 1). Both systems were also confirmed to have relatively low polydispersity (0.06 and 0.05 for NC-PFPMA and NC-*t*BMA, respectively). The subsequent IMEPP reaction was able to

dx.doi.org/10.1021/mz5005019 | *ACS Macro Lett.* 2014, 3, 935−939

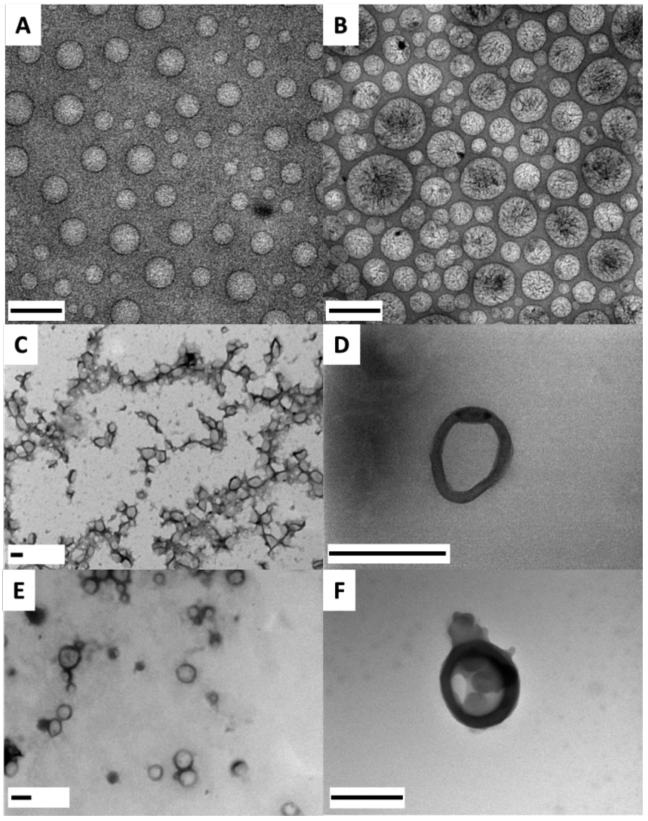

Figure 1. Cryo-TEM micrographs of the initial (before polymerization) inverse miniemulsions stabilized by PHPMA-*b*-P*t*BMA (A) or PHPMA-*b*-PPFPMA (B). TEM micrographs of NC-PFPMA (C) and NC-*t*BMA (D) synthesized via IMEPP; TEM micrographs of the modified nanocapsules, NC−COOH (E) and NC-amine (F). Scale bar is 200 nm.

preserve the low polydispersity of the systems, as shown by the DLS results of the raw emulsion (IMEPP; Table 1). After purification, the nanocapsules were redispersed in toluene and DMAc. Redispersion in toluene revealed the presence of nanocapsules with similar sizes to that of the raw emulsion, *Z*-avg. = 234 nm and 241 (NC-*t*BMA and NC-PFPMA, respectively). These results confirmed that the synthesized shells were able to preserve the original size of the droplet templates. The relatively low polydispersity values demonstrated the stability of the synthesized nanocapsules, even after drying and redispersion in various solvents.

The purified nanocapsules were also redispersed in DMAc to confirm the integrity of the polymeric shells. DMAc was chosen as it is a common solvent for both the hydrophilic and the hydrophobic segment of the block copolymers. In this case, if the polymeric shell was not cross-linked, it would disintegrate into the individual polymeric chains. The results showed nanocapsules with similar sizes to that from the redispersion in toluene, with the small discrepancies attributed to the polymeric chains behavior in different solvent. The absence of any peaks that represent unimolecularly dissolved polymeric chains, together with the low PDI value of the systems, confirmed the success of the cross-linking reaction. All DLS results also revealed monomodal distributions (SI, Figure S3), which further iterate the efficacy of the IMEPP process.

TEM micrographs of both nanocapsules showed the distinctive hollow core (light) and spherical polymeric shell (dark) morphology. From the micrographs (Figure 1 and SI, Figure S4), the measured diameters of NC-*t*BMA and NC-PFPMA were 191 and 210 nm, respectively. The shell thicknesses were measured to be 21 and 31 nm, respectively. These results are comparable to the calculated shell thicknesses from DLS (*Z*-avg.) of 26 and 30 nm, respectively (shell thickness = ($Z\text{-avg.}_{\text{IMEPP}} - Z\text{-avg.}_{\text{initial miniemulsion}}$)/2). The shell thicknesses were also theoretically calculated according to the method described elsewhere.[39] The measured shell thicknesses were confirmed to be well within the theoretically calculated range of between 9 and 50 nm for NC-*t*BMA and 17 and 36 nm for NC-PFPMA. The small variations of the results between different analysis techniques are attributed to the flexibility characteristic of the polymeric shells depending on the surrounding environment.

Table 1. DLS Results for Both NC-*t*BMA and NC-PFPMA Showing the Diameters and the PDI of the Initial Droplets (Initial Miniemulsion), Final Product Prior to Purification (IMEPP), Redispersion of the Purified Nanocapsules in Toluene (in Toluene) and in DMAc (in DMAc), and the Redispersion of the Modified Nanocapsules in Water (Modified Capsules)

sample name		*Z*-avg.[a] (nm)	d_n[b] (nm)	d_i[c] (nm)	d_v[d] (nm)	PDI[e]
initial miniemulsion	NC-*t*BMA	167	151	177	184	0.05
	NC-PFPMA	206	193	220	238	0.06
IMEPP	NC-*t*BMA	219	196	242	272	0.09
	NC-PFPMA	265	259	304	333	0.06
in toluene	NC-*t*BMA	234	189	268	298	0.12
	NC-PFPMA	241	211	280	328	0.17
in DMAc	NC-*t*BMA	208	185	224	241	0.06
	NC-PFPMA	211	185	224	253	0.10
modified capsules in water	NC-COOH	258	224	241	250	0.21
	NC-amine	213	166	240	259	0.11

[a]*Z*-average diameter. [b]Number-average diameter. [c]Intensity average diameter. [d]Volume average diameter. [e]Polydispersity index.

Two different pathways were used to produce pH-responsive nanocapsules (Scheme 1). For the modification NC-*t*BMA (to produce NC−COOH), acid hydrolysis of the *tert*-butyl protective group was conducted with TFA at room temperature. The completeness of the reaction was analyzed by ^{1}H NMR by monitoring the disappearance of the *tert*-butyl signal 1.5 ppm (SI, Figure S5). A shift of the methyl signal on the backbone was also observable on the deprotected nanocapsules due to the presence of carboxylic acid functionality (SI, Figure S5). In contrast, pH-responsive nanocapsules bearing amine functionality (NC-amine) were obtained via aminolysis of the activated ester group with DMAPA. The completion of the reaction was confirmed by ^{19}F NNR by monitoring the disappearance of the PPFPMA signal from the polymer and the appearance of the pentafluorophenol signal as the byproduct (SI, Figure S6). In addition, ^{1}H NMR reveals the presence of the appropriate alkyl functionalities confirming complete functionalization (SI, Figure S7).

dx.doi.org/10.1021/mz5005019 | *ACS Macro Lett.* 2014, 3, 935−939

DLS analyses of the modified nanocapsules were carried out in water. The nanocapsules were found to be readily dispersed in water. This was in contrast to the initial nanocapsules, which were only dispersible in nonpolar solvents and would aggregate and precipitate in water. For both types of nanocapsules, there was no change in the stability of the nanocapsules, as evidenced by the monomodal distribution and the low PDI values from the DLS analysis (SI, Figure S3). From the TEM micrographs obtained (Figure 1 and SI, Figure S8), both nanocapsules were confirmed to retain their core−shell morphology.

From the DLS results, an increase in nanocapsule diameter was observed when NC-*t*BMA (*Z*-Avg. = 208 nm) was hydrolyzed into NC-COOH (*Z*-Avg. = 258 nm). This trend was also observed from the TEM micrographs. The measured diameter of NC-COOH was 238 nm, with a shell thickness of 44 nm, larger than diameter (191 nm) and the shell thickness (21 nm) of the initial NC-*t*BMA. In contrast, the resulting NC-amine (*Z*-avg. = 213 nm) showed no significant changes on the size when compared to the initial NC-PFPMA (*Z*-Avg. = 211 nm). TEM analysis showed nanocapsules with a diameter of 222 nm, comparable to the DLS result. The shell thickness was measured to be 36 nm which is very similar to the measured thickness of 31 nm on NC-PFPMA. The different behaviors observed further confirmed successful modification of the polymeric shells and gave an early indication of their responsive behavior. Both the DLS and the TEM results confirmed that the postpolymerization reactions proceed efficiently and did not have any impact on the morphology and the stability of the nanocapsules, while the observed change in size is correlated to the successful introduction of responsive functionalities into the shell.

Controlled release of encapsulated agents through a change in pH has been well documented and exploited. Herein, we report the efficient production of two different types of pH-responsive nanocapsules which display opposite behavior when dispersed in acidic or basic aqueous solutions. The change in size was analyzed via DLS and the *Z*-average values were used to give a close representation of the trend (Table S3).

NC-COOH experienced an increase in size as the pH of the solution was increased (Figure 2). This is attributed to the deprotonation of the carboxylic acid groups, which promote the electrorepulsive forces between the carboxylate ions within the chains. The surface charge of NC-COOH at neutral pH was confirmed to be negative due to the deprotonation of the carboxylic acid groups. As the pH increased, the zeta-potential decreased further until the most negative zeta-potential was reached between 7 and 10, coinciding with the full deprotonation. Once this pH regime has been reached, no further increase in particle size was observed (Figure 2). As expected, protonation occurred as the pH was decreased, represented by the increase in zeta potential and reaching a positive value (+13 mV) at pH 3.

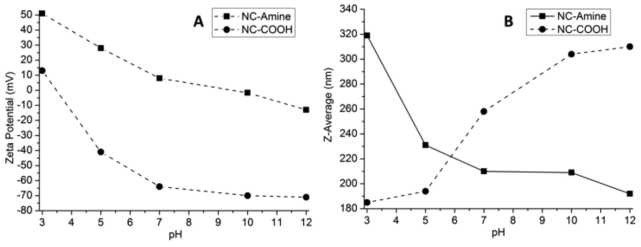

Figure 2. Plots correlating the change in zeta-potential (A) and *Z*-average size (B) with the change in pH of NC-amine (square) and NC-COOH (circle).

NC-amine showed the opposite behavior to that of NC-COOH. In this case, the nanocapsule diameter was found to decrease as the pH was increased due to the protonation of the amine functionality at low pH. As a result, repulsive forces between the positive charges cause the polymeric shell to swell. At neutral pH, the surface was found to be slightly positive (+8 mV) due to slight protonation, which was expected considering the pK_a value of the tertiary amine at 7.7.[40] Protonation led not only to the increase of the zeta potential (up to +51 mV at pH 3), but also the increase in particle size due to repulsive forces. Negative zeta potential values were recorded when the pH of the solution was adjusted to 12. This could be attributed to other functionalities present within the shell, such as the hydroxyl from the PHPMA chain. However, the contribution of this to the size of the nanocapsules was confirmed to be insignificant. For both NC-COOH and NC-amine, the PDI values decreased with an increasing level of charge (i.e., with increasing absolute value of the zeta potential). This is attributed to electrostatic repulsive forces leading to improved colloidal stabilization and, thus, less aggregation. The presented behavior of these nanocapsules could thus be exploited to selectively control the release rate of encapsulated molecules; an expanded, less dense shell would be anticipated to result in a higher release rate due to lower diffusion resistance.

Two different types of pH-responsive nanocapsules have been successfully synthesized through IMEPP and postpolymerization reactions. IMEPP of both *t*BMA and PFPMA were performed initially to produce polymeric nanocapsules. For polymeric nanocapsules having *t*BMA shell (NC-*t*BMA), acid-catalyzed hydrolysis was conducted to yield polymeric nanocapsules with anionic, pH-responsive, methacrylic acid shells (NC-COOH). In contrast, polymeric nanocapsules with PFPMA (NC-PFPMA) shell underwent aminolysis to generate cationic *N*-[3-(dimethylamino)propyl] methacrylamide shells (NC-amine). The IMEPP reaction and the postpolymerization reaction were both confirmed to have no influence on the size and the stability of droplets/nanocapsules.

The pH responsiveness of the nanocapsules was confirmed over the pH range from 3 to 12. For NC-COOH, the shell swelled under basic conditions due to the deprotonation of the carboxylic acid functionality. This was also confirmed by the negative zeta-potential value representing the negatively charged carboxylate ion. In contrast, NC-amine shell swelled under acidic conditions due to the protonation of the amine functionality confirmed by the positive zeta-potential value. It is envisaged that the tunable degree of swelling of the shells can be exploited for control of the release rates of encapsulated drugs. Furthermore, with the current report on the versatility of IMEPP and postpolymerization reaction, we believe that this methodology can be exploited further to introduce various functionalities to suit particular applications.

■ ASSOCIATED CONTENT

Supporting Information

Materials and detailed experimental procedures; GPC analysis of the polymers; TEM and cryo-TEM micrographs; NMR analyses of the postfunctionalization. This material is available free of charge via the Internet at http://pubs.acs.org.

dx.doi.org/10.1021/mz5005019 | *ACS Macro Lett.* 2014, 3, 935−939

AUTHOR INFORMATION

Corresponding Authors

*E-mail: m.stenzel@unsw.edu.au.

*E-mail: p.zetterlund@unsw.edu.au.

Notes

The authors declare no competing financial interest.

ACKNOWLEDGMENTS

The authors acknowledge the Australian Research Council. R.H.U. would like to thank the UNSW student exchange office for a Student Exchange Scholarship.

REFERENCES

(1) Du, P.; Mu, B.; Wang, Y.; Shi, H.; Xue, D.; Liu, P. *Mater. Lett.* **2011**, *65* (11), 1579−1581.

(2) Gao, H.; Yang, W.; Min, K.; Zha, L.; Wang, C.; Fu, S. *Polymer* **2005**, *46* (4), 1087−1093.

(3) Chécot, F.; Rodríguez-Hernández, J.; Gnanou, Y.; Lecommandoux, S. *Biomol Eng.* **2007**, *24* (1), 81−85.

(4) Sauer, M.; Meier, W. *Chem. Commun.* **2001**, No. 1, 55−56.

(5) Gu, W. F.; Ting, S. R. S.; Stenzel, M. H. *Polymer* **2013**, *54* (3), 1010−1017.

(6) Cui, J.; Fan, D.; Hao, J. *J. Colloid Interface Sci.* **2009**, *330* (2), 488−492.

(7) Falqueiro, A. M.; Primo, F. L.; Morais, P. C.; Mosiniewicz-Szablewska, E.; Suchocki, P.; Tedesco, A. C. *J. Appl. Phys.* **2011**, *109* (7), 07B306.

(8) Staff, R. H.; Gallei, M.; Mazurowski, M.; Rehahn, M.; Berger, R.; Landfester, K.; Crespy, D. *ACS Nano* **2012**, *6* (10), 9042−9049.

(9) Zhao, M.; Biswas, A.; Hu, B.; Joo, K.-I.; Wang, P.; Gu, Z.; Tang, Y. *Biomaterials* **2011**, *32* (22), 5223−5230.

(10) Gupta, P.; Vermani, K.; Garg, S. *Drug Discovery Today* **2002**, *7* (10), 569−579.

(11) Lackey, C. A.; Murthy, N.; Press, O. W.; Tirrell, D. A.; Hoffman, A. S.; Stayton, P. S. *Bioconjugate Chem.* **1999**, *10* (3), 401−405.

(12) Stuart, M. A. C.; Huck, W. T. S.; Genzer, J.; Muller, M.; Ober, C.; Stamm, M.; Sukhorukov, G. B.; Szleifer, I.; Tsukruk, V. V.; Urban, M.; Winnik, F.; Zauscher, S.; Luzinov, I.; Minko, S. *Nat. Mater.* **2010**, *9* (2), 101−113.

(13) Gao, W.; Chan, J. M.; Farokhzad, O. C. *Mol. Pharmaceutics* **2010**, *7* (6), 1913−1920.

(14) Schmaljohann, D. *Adv. Drug Delivery Rev.* **2006**, *58* (15), 1655−1670.

(15) Riedinger, A.; Pernia Leal, M.; Deka, S. R.; George, C.; Franchini, I. R.; Falqui, A.; Cingolani, R.; Pellegrino, T. *Nano Lett.* **2011**, *11* (8), 3136−3141.

(16) Ruan, C.; Zeng, K.; Grimes, C. A. *Anal. Chim. Acta* **2003**, *497* (1−2), 123−131.

(17) Hester, J. F.; Olugebefola, S. C.; Mayes, A. M. *J. Membr. Sci.* **2002**, *208* (1−2), 375−388.

(18) Ito, Y.; Ochiai, Y.; Park, Y. S.; Imanishi, Y. *J. Am. Chem. Soc.* **1997**, *119* (7), 1619−1623.

(19) Johnston, A. P. R.; Cortez, C.; Angelatos, A. S.; Caruso, F. *Curr. Opin. Colloid Interface Sci.* **2006**, *11* (4), 203−209.

(20) Samad, A.; Sultana, Y.; Aqil, M. *Curr. Drug Delivery* **2007**, *4* (4), 297−305.

(21) Chen, B.-Y.; Huang, Y.-F.; Huang, Y.-C.; Wen, T.-C.; Jan, J.-S. *ACS Macro Lett.* **2014**, *3* (3), 220−223.

(22) Song, J.; Zhou, J.; Duan, H. *J. Am. Chem. Soc.* **2012**, *134* (32), 13458−13469.

(23) Du, J.; Armes, S. P. *J. Am. Chem. Soc.* **2005**, *127* (37), 12800−12801.

(24) Yoshida, M.; Takimoto, R.; Murase, K.; Sato, Y.; Hirakawa, M.; Tamura, F.; Sato, T.; Iyama, S.; Osuga, T.; Miyanishi, K.; Takada, K.; Hayashi, T.; Kobune, M.; Kato, J. *PLoS One* **2012**, *7* (7), e39545.

(25) Ali, S. I.; Heuts, J. P. A.; van Herk, A. M. *Soft Matter* **2011**, *7* (11), 5382−5390.

(26) Liu, Y.; Yang, J.; Zhao, Z.; Li, J.; Zhang, R.; Yao, F. *J. Colloid Interface Sci.* **2012**, *379* (1), 130−140.

(27) Shu, S.; Zhang, X.; Wu, Z.; Wang, Z.; Li, C. *Biomaterials* **2010**, *31* (23), 6039−6049.

(28) Thomas, M. B.; Radhakrishnan, K.; Gnanadhas, D. P.; Chakravortty, D.; Raichur, A. M. *Int. J. Nanomed.* **2013**, *8*, 267.

(29) Ye, S.; Wang, C.; Liu, X.; Tong, Z. *J. Biomater. Sci., Polym. Ed.* **2005**, *16* (7), 909−923.

(30) Gu, X.; Wang, J.; Wang, Y.; Wang, Y.; Gao, H.; Wu, G. *Colloids Surf., B* **2013**, *108* (0), 205−211.

(31) Li, W.; Yoon, J. A.; Matyjaszewski, K. *J. Am. Chem. Soc.* **2010**, *132* (23), 7823−7825.

(32) Luo, Y.; Gu, H. *Polymer* **2007**, *48* (11), 3262−3272.

(33) Paiphansiri, U.; Dausend, J.; Musyanovych, A.; Mailänder, V.; Landfester, K. *Macromol. Biosci.* **2009**, *9* (6), 575−584.

(34) Rosenbauer, E.-M.; Landfester, K.; Musyanovych, A. *Langmuir* **2009**, *25* (20), 12084−12091.

(35) Roux, R.; Sallet, L.; Alcouffe, P.; Chambert, S.; Sintes-Zydowicz, N.; Fleury, E.; Bernard, J. *ACS Macro Lett.* **2012**, *1* (8), 1074−1078.

(36) Siebert, J. M.; Baier, G.; Musyanovych, A.; Landfester, K. *Chem. Commun.* **2012**, *48* (44), 5470−5472.

(37) Cao, Z.; Landfester, K.; Ziener, U. *Langmuir* **2011**, *28* (2), 1163−1168.

(38) Utama, R. H.; Guo, Y.; Zetterlund, P. B.; Stenzel, M. H. *Chem. Commun.* **2012**, *48* (90), 11103−11105.

(39) Utama, R. H.; Stenzel, M. H.; Zetterlund, P. B. *Macromolecules* **2013**, *46* (6), 2118−2127.

(40) Agut, W.; Brûlet, A.; Schatz, C.; Taton, D.; Lecommandoux, S. b. *Langmuir* **2010**, *26* (13), 10546−10554.